Two-Dimensional Regular Nanopatterning on Block Copolymer Substrate Having Lamellar Morphology Using Star-Hyperbranched Nanospheres by Electrostatic Interaction

Koji Ishizu,[1] Koichiro Ochi,[1] Satoshi Uchida,[1] Keisuke Odoi[2]

[1]*Department of Organic Materials and Macromolecules, International Research Center of Macromolecular Science, Tokyo Institute of Technology, Tokyo 152-8552, Japan*
[2]*Nissan Chemical Industries Ltd., 7–1, 3-Chome, Kanda-Nishiki-cho, Chiyoda-ku, Tokyo 101-0054, Japan*

Received 21 March 2005; accepted 21 September 2005
DOI 10.1002/app.23632
Published online in Wiley InterScience (www.interscience.wiley.com).

ABSTRACT: Hyperbranched polystyrenes (PS) were prepared by living radical photopolymerization of 4-vinylbenzyl *N*,*N*-diethyldithiocarbamate as an inimer under UV irradiation. The star-hyperbranched copolymers were derived by grafting from surface *N*,*N*-diethyldithiocarbamate groups of hyperbranched macroinitiator with *t*-butyl methacrylate in the presence of *N*,*N*-tetraethylthiuram disulfide. We obtained poly(methacrylic acid) star-hyperbranched PS nanospheres by hydrolysis of poly(*t*-butyl methacrylate)-grafted chains. We established two-dimensional (2D) regular nanopatterning by aligning continuously such nanospheres on poly(2-vinylpyridine) (P2VP) lamellar layers of PS-*block*-P2VP diblock copolymer film. Electrostatic interaction between nanosphere surface having negative charges (—COOCs) and P2VP lamellar layer acted effectively for the 2D nanopattern formation. © 2006 Wiley Periodicals, Inc. J Appl Polym Sci 101: 4206–4210, 2006

Key words: living radical polymerization; star-hyperbranched nanosphere; nanopatterning; block copolymer; electrostatic interaction

INTRODUCTION

There has been a strong interest in the self-assembly of particles utilizing driving forces, such as electrostatic interactions, surface tension, van der Waals forces, and capillary force, to create ordered structures into two and three dimensions. Electrostatic interactions have been widely employed in the assembly of particles ranging from micro- to nanoscale dimensions.[1–7] Otsu and coworkers reported that the polymerization of vinyl monomers with mono- and bifunctional photoinitiators having *N*,*N*-diethyldithiocarbamate (DC) groups proceeded via a living radical mechanism.[8,9] More recently, we succeeded in two-dimensional (2D) nanopatterning of poly(methacrylic acid) (PMA) star-hyperbranched polystyrene (PS) nanospheres on partially quaternized poly(4-vinylpyridine) (P4VP) substrate by electrostatic interaction.[10] We also presented a novel route of such star-hyperbranched copolymers by a living radical mechanism (see Scheme 1).[11] That is to say, one-pot photopolymerization of 4-vinylbenzyl *N*,*N*-diethyldithiocarbamate (VBDC) provided hyperbranched PS.[12] We could prepare subsequently star-hyperbranched copolymers by graft photopolymerization with other vinyl monomers, because the hyperbranched polymer has large amounts of photofunctional DC groups on its outside surface.

On the other hand, thin films of block copolymers are to be well ordered to provide the highest density of the domains and an equal distance between them. Krausch and coworkers[13] proposed an alternative method to promote self-assembly into nanometer-scale domains. The procedure consists of the controlled swelling of block copolymer thin films in solvent vapor. Solvent quality and swelling ratio may affect the morphology and, particularly, orientation of nanoscopic domains in films of triblock copolymers. Very recently, an approach was suggested by Kramer and coworkers.[14] They explored the phenomenon of topographical confinement (lithographically patternal Si-wafer) to introduce a single crystalline order in a single layer of block copolymer spheres. It is interesting to establish the 2D regular nanopatterning using hyperbranched nanospheres on the lamellar layers of block copolymer films for the application of various kinds of devices

In this article, poly(*t*-butyl methacrylate) (PBMA) star-hyperbranched PS nanospheres were prepared by

Correspondence to: K. Ishizu (kishizu@polymer.titech.ac.jp).

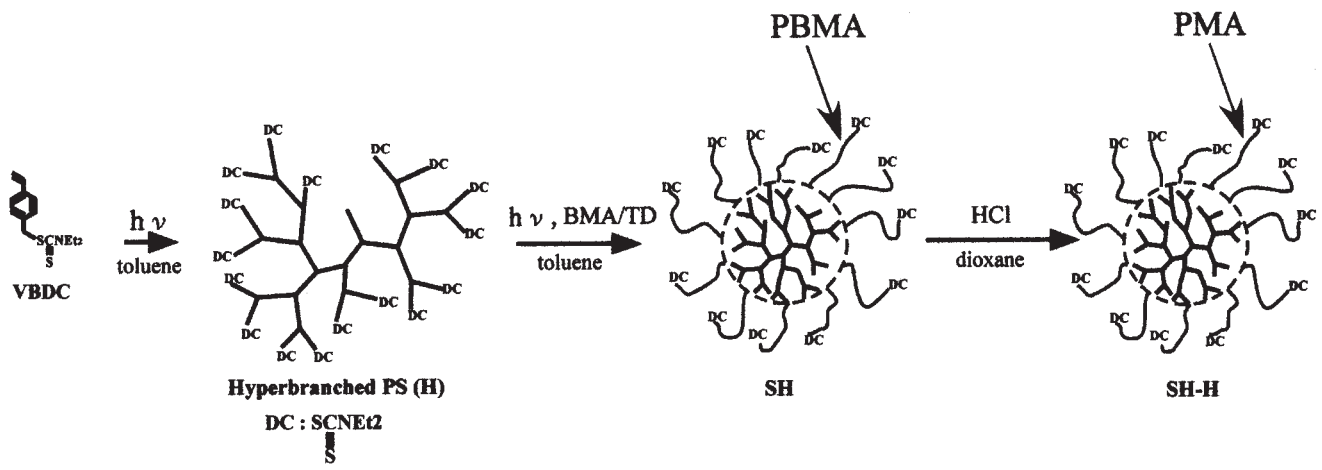

Scheme 1

living radical photopolymerization. After hydrolysis of PBMA grafted chains, we obtained PMA star-hyperbranched PS copolymers. These copolymers formed single nanospherical molecules in methanol or an alkaline aqueous solution. We studied the 2D regular nanopatterning on PS-*block*-poly(2-vinylpyridine) (P2VP) film having lamellar morphology using nanospheres with surface negative charges by electrostatic interaction. Nanopattern formation was observed directly by transmission electron microscopy (TEM).

EXPERIMENTAL

Materials

VBDC was synthesized by the reaction of *p*-chloromethylstyrene (Seimi Chemical Industry) with *N*,*N*-diethyldithiocarbamate sodium salt (DCNa) (Tokyo Kasei Organic Chemicals) in acetone. Details concerning the synthesis and purification of VBDC have been given elsewhere.[12] BMA (Tokyo Kasei Organic Chemicals) was distilled under high vacuum. *N*,*N*-Tetraethylthiuram disulfide (TD), toluene, tetrahydrofuran (THF), dioxane, methanol, methyl iodide, HCl, and cesium hydroxide (CsOH) (Tokyo Kasei Organic Chemicals) were used as received. PS-*block*-P2VP diblock copolymer was synthesized by living anionic polymerization technique initiated by *n*-butyl lithium in THF. Details concerning the synthesis and characterization of diblock copolymer were given elsewhere.[15]

Synthesis and characterization of hyperbranched polymers and star-hyperbranched copolymers

Photopolymerizations of VBDC (50 wt % toluene solution) were carried out by irradiation with UV light, in a sealed Pyrex glass ampoule for 6 h under high vacuum at 30°C. The precipitation fractionation of hyperbranched PS was carried out with a toluene–methanol system, because the hyperbranched PS exhibited a broad molecular-weight distribution. Details concerning the apparatus and its conditions have been given elsewhere.[11,12]

The star-hyperbranched copolymers were prepared by graft photocopolymerization of hyperbranched macroinitiator with BMA, in the presence of TD in toluene under 8 h of UV irradiation time ([BMA]/[DC] = 50 (mol/mol), [TD]/[DC] = 2 (mol/mol), 28 vol % monomer concentration). Subsequently, we obtained PMA star-hyperbranched PS copolymers by hydrolysis of PBMA grafted chains in dioxane using HCl (refluxing for 5 h). Details concerning hydrolysis have been also given elsewhere.[10]

The weight-average molecular weights (M_w) and hydrodynamic radius (R_h) of hyperbranched PS and PBMA star-PS hyperbranched copolymer were determined by static and dynamic light scatterings (SLS and DLS; Photal TMLS-6000HL, Otsuka Electronics) with an He–Ne laser (λ_0 = 632.8 nm), respectively, in toluene at 25°C. R_h of PMA star-hyperbranched PS was also determined by DLS with cumulant method in methanol at 25°C. Sample solutions were filtered through membrane filters with a nominal pore size of 0.2 μm just before measurement. The radius of gyration (R_g) of star-hyperbranched copolymer was also determined in toluene by SLS with Zimm mode. The refractive index increments (dn/dc) were determined by refractometer and each value is listed in Table I, as described later. Details concerning apparatus and measurement conditions have been given elsewhere.[10] R_g of hyperbranched PS prepared from this work was very small. Thus R_g was determined by small-angle X-ray scattering (SAXS). The SAXS intensity distribution $I(q)$ was measured with a rotating-anode X-ray generator (Rigaku Denki Rotaflex RTC 300RC) operated at 40 kV and 100 mA. The X-ray source was

TABLE I
Characteristics of Hyperbranched PS (HF) and PBMA Star-PS Hyperbranched Copolymers (SH)[a]

Code	dn/dc[b] (mL/g)	$10^{-4}\ M_w^c$	M_w/M_n^d	R_h^c (nm)	$R_g^{c,F}$ (nm)	DP_n^g
HF	0.181	8.0	1.37	4.4	3.8	
SH1	0.021	155	1.36	14.0	12.3	34

[a] UV irradiation time (8 h) for SH1 in the presence of TD.
[b] Refractive index increments of HF and SH were measured in toluene.
[c] Determined by SLS in toluene with Zimm mode at 25°C.
[d] Determined by GPC with THF as eluent at 38°C using calibration of PS standard samples.
[e] Determined by DLS in toluene with cumulant method at 25°C.
[g] Degree of polymerization of PBMA grafted chain.
[F] Determined in toluene by Guinier's plot on SAXS.

monochromatic Cu Kα (λ = 15.4 nm) radiation. In the measurement of a toluene solution (1 wt %) of the sample, we used the cell sandwiched between mica plates as a holder vessel. The background correction was carried out using polyethylene film. The value of R_g is estimated by Guinier's method from the following equation.[16]

$$\ln I(q) = \text{constant} - (1/3)(R_g^2)q^2$$

where q is the scattering vector.

The molecular weight distributions of hyperbranched polymers and star-hyperbranched copolymers were determined by gel permeation chromatography (GPC; Tosoh high-speed liquid chromatograph HLC-8020) using PS standard samples in THF as the eluent at 38°C, two TSK gel columns, GMHXL [excluded-limit molecular weight (MEL = 4.8 × 108)], and G2000HHL (MEL = 1 × 104), in series and a flow rate of 1.0 mL/min

2D nanopatterning on block copolymer substrate

Thomas and O'Malley[17] have investigated the surface properties of block copolymers and, in particular, their surface composition and topography at the air–copolymer interface. They have made clear that the surface and bulk were not identical because of significant differences in the solid-state surface tension of each block. In general, the thermal equilibrium morphology of symmetric diblock copolymers was horizontally oriented lamellar microdomains not only near the upper and lower film surfaces but also in bulk.[18–21] PS-*block*-P2VP diblock copolymer (SV) film (40-μm thick) was cast from a 0.03 g/mL THF solution, with a Teflon sheet (0.11 mL/cm^2) as a substrate. The casting solvent was evaporated as gradually as possible under saturated vapor. Next, the films were embedded in an epoxy resin and cut perpendicularly to the film interfaces into ultrathin sections (about 70–100 nm thick), using an ultramicrotome (Reichert-Nissei Co., Ultracut N). P2VP domains were selectively stained with CH3I vapor. Morphological results were obtained by TEM on a Hitachi H-500 operated at 75 kV. To estimate the periodic distance of lamellae, we also carried out SAXS measurement of SV film. The SAXS intensity profiles were plotted from the horizontal section of the SAXS patterns without considering the smearing correction.

Nanopattern formation was performed as follows. The thin SV film sections as substrates were picked up on a copper grid. A 0.5 wt % water/methanol 6/4 (v/v) mixture of PMA star-hyperbranched PS nanospheres neutralized with CsOH was dropped on such polymer substrate and the solvent was evaporated as slowly as possible at 25°C. Each specimen was washed well with several drops of corresponding mixed solution. Nanopattern formation of nanospheres was observed directly by TEM for such specimens.

RESULTS AND DISCUSSION

Synthesis and solution properties of hyperbranched and star-hyperbranched copolymers

Photopolymerization of VBDC provided hyperbranched PS. Since its polydispersity was broad, the precipitation fractionation of the product was carried out in a toluene–methanol system. A GPC profile of the hyperbranched PS fraction HF is shown in Figure 1. The values of M_w (8.0 × 10^4) and M_w/M_n (1.37) determined from SLS and GPC, respectively, are listed in Table I. To understand the inner density profile, it is important to determine the degree of branching (DB) of hyperbranched PS. Because the primary benzylic

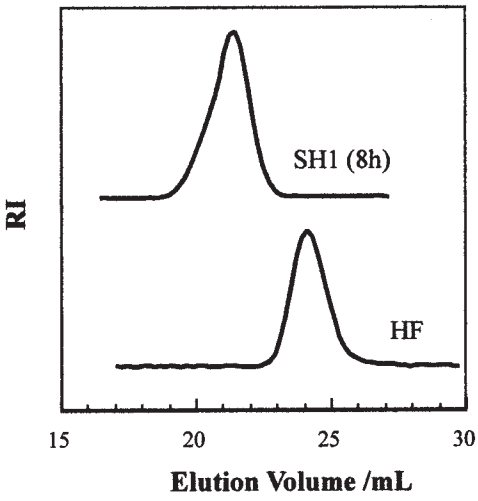

Figure 1 GPC profiles of hyperbranched PS (HF) and PBMA star-PS hyperbranched copolymers (SH1) in THF as an eluent at 38°C.

DC group (B*) on VBDC monomer unit may be much less reactive than the secondary benzylic DC group (A) formed after initiation, the polymer obtained by photopolymerization of VBDC possibly have very limited branching. So, we treated the kinetics of initiation and propagation steps of the active A* and B* (side group) sites using model compounds.[22] As a result, the DB of hyperbranched PS was estimated to be 0.31 using both reaction rates in terms of Müller's equation.[23] This result supported the DB (0.39) estimated from NMR data.[24] Hyperbranched molecules were not perfectly dendritic but somewhat defective structures. R_h (4.4 nm) was estimated using Stokes–Einstein equation, after the diffusion coefficient (D_0) was determined by extrapolation of DLS data to zero concentration with cumulant method. As mentioned in the previous work,[8] the ratio R_g/R_h is a sensitive fingerprint of the inner density profile of star molecules and polymer micelles. The hyperbranched PS HF prepared in this work with higher inner density ($R_g/R_h = 0.86$) seems to behave as a hard sphere ($R_g/R_h = 0.775$) in the dilute solution.

PBMA star-hyperbranched PS copolymers were prepared by graft copolymerization of HF macroinitiator and BMA. Photopolymerization led to partial gelation after 10 min of UV irradiation, especially in the case of high DC concentration. So, we carried out such graft copolymerization in the presence of TD. Typical GPC profiles of the copolymers are also shown in Figure 1. GPC curves of SH1 (8 h) shows a unimodal distribution and elution peaks of GPC shift to the high-molecular-weight side than that of hyperbranched PS HF. The molecular weight distribution ($M_w/M_n = 1.36$) is almost the same as that of starting macroinitiator HF. It is the dynamic equilibrium that is responsible for the controlled behavior of the polymerization of BMA. It seems that the reverse coupling rate between the dormant polymer chains and DC radicals is rapid due to high concentration of DC radicals. The degree of polymerization ($DP_n = 34$) of a PBMA grafted chain was calculated from the molecular weight of PBMA and the number of DC (301 per molecule), assuming that BMA monomers propagated from all the DC groups on the outside surface of the hyperbranched macroinitiator HF. We expected the determination of the initiator efficiency after graft polymerization by ^{13}C NMR to distinguish primary and secondary benzylic carbons connected to the DC functionality. However, both signals were not observed due to higher molecular weight of PBMA grafted chains.

As mentioned in the previous paper,[25] PBMA star-PS hyperbranched copolymers also did not show an angular dependence of $\Gamma_e q^{-2}$ on q from DLS data in toluene (Γ_e: the first cumulant, q: scattering vector), and the mutual diffusion coefficient $D(C)$ had a constant value in the range 4–15 mg/mL of polymer concentration. Then, these copolymers formed nanospherical particles ($R_h = 14.0$ nm) even in a good solvent.

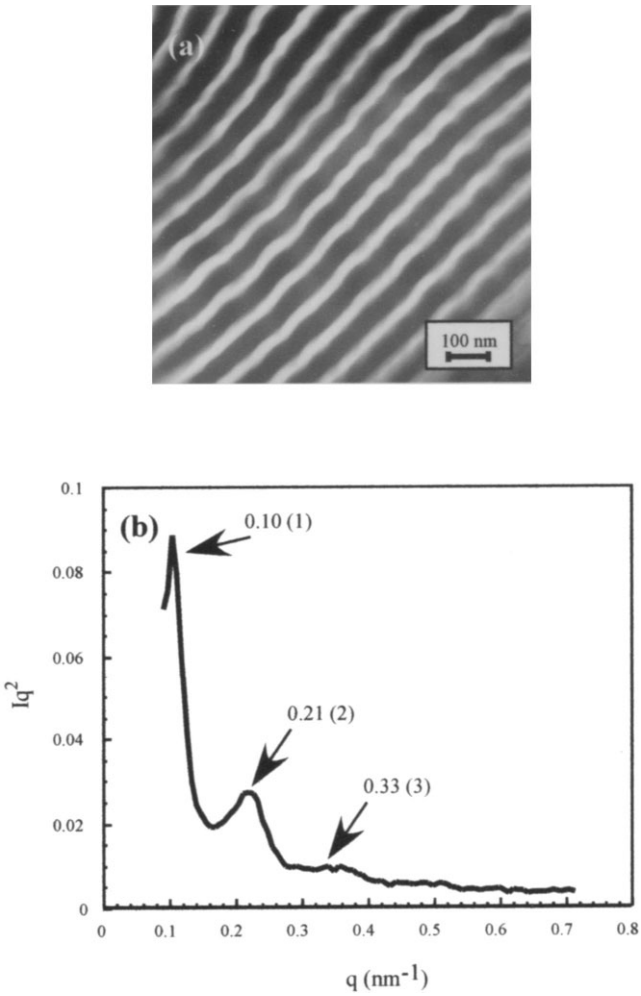

Figure 2 TEM photograph (a) and SAXS intensity profile (b) of PS-*block*-P2VP diblock copolymer.

At last, we carried out the hydrolysis of PBMA grafted chains using HCl followed by the procedure described in the previous paper.[8] The SH copolymers could be derived to PMA star-PS hyperbranched copolymers (SH-H). The SH1H copolymer ($DP_n = 34$) was soluble in methanol or an alkaline aqueous solution. R_h of SH1H was evaluated to be 12.6 nm by DLS in methanol. This value was in agreement with that ($R_h = 14.0$ nm) of SH1 in toluene within experimental error.

2D regular nanopatterning of nanospheres on polymer substrate

Figure 2(a) shows the TEM photograph of PS-*block*-P2VP copolymer specimen ($M_n = 8.53 \times 104$, PS 43 wt %). The dark portions are the selectively stained P2VP blocks with CH3I. This specimen shows the texture of

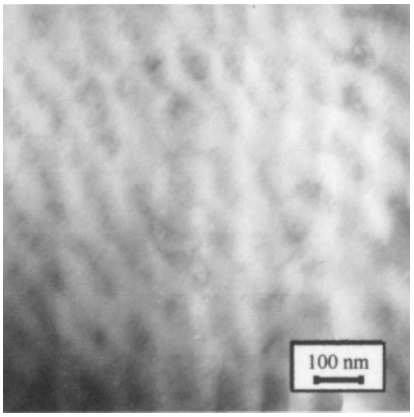

Figure 3 TEM photograph of 2D regular nanopatterning of nanospheres SH1H-Cs on PS-*block*-P2VP diblock copolymer substrate.

alternating PS/P2VP lamellar morphology due to symmetric structure. Figure 2(b) shows the SAXS intensity profile of the SV film at the edge view, where q [$= (4\pi/\lambda)\sin\theta$] is the magnitude of the scattering vector. The arrows show the scattering maxima and the values indicate the scattering vectors. On the other hand, the values in parentheses indicate the interplanar spacings (d_1/d_i) calculated from Bragg reflections. The first three peaks are observed at the relative q positions of 1:2:3, as shown by arrows. The interplanar spacings at the scattering angles is relative to the angle of the first maximum according to Bragg equation: $2d \sin\theta = \lambda$ (where θ is half the scattering angle, $\lambda = 15.4$ nm). This packing pattern corresponds to lamellar morphology. Periodic distance of lamellae is estimated to be 62 nm. The distance of P2VP lamellae was estimated to be 40 nm from TEM photograph [Fig. 2(a)]. This value depends strongly to the cutting angle of SV film embedded in an epoxy resin.

To construct the 2D regular nanopattern, the dilute mixed solution of SH1H-Cs was dropped on PS-*block*-P2VP diblock copolymer film and washed well with corresponding mixed solution. Figure 3 shows TEM photograph of nanopatterning film. We can directly observe nanospheres because the shell of SH1H-Cs was composed of heavy Cs metals. The dark portions (stripe distance = 23–28 nm) correspond to SH1H-Cs nanospheres. It is found from this TEM image that one nanosphere aligned continuously and regularly on P2VP lamellar layers, because the periodic distance (40 nm) of P2VP lamellae is significantly larger than the sizes of polymeric particles (hydrodynamic diameter D_h = 25.2 nm). This may be indicated by the collapsed structures of SH1H-Cs on the P2VP lamellar surface. It means that electrostatic interaction between nanosphere surface having negative charges (—COOCs) and P2VP lamellar layers acts effectively for the 2D nanopattern formation.

CONCLUSIONS

PMA star-PS hyperbranched copolymers were prepared by living radical photopolymerization. These copolymers behaved as nanospheres in methanol or in alkaline aqueous solution. We established the 2D regular nanopatterning by aligning continuously such nanospheres on P2VP lamellar layers of PS-*block*-P2VPQ diblock copolymer film. Electrostatic interaction between nanosphere surface having negative charges (—COOCs) and P2VP lamellar layers acted effectively for the 2D nanopattern formation.

References

1. Tien, J.; Terfort, A.; Whitesides, G. Langmuir 1997, 13, 5349.
2. Serizawa, T.; Takeshita, H.; Akashi, M. Langmuir 1998, 14, 4088.
3. Schmitt, J.; Machtle, P.; Eck, D.; Mohwald, H.; Helm, C. A. Langmuir 1999, 15, 3256.
4. Yonezawa, T.; Onoue, S.; Kunitake, T. Chem Lett 1998, 27, 689.
5. Schmitt, J.; Decher, G.; Dressick, W. J.; Brandow, S. L.; Geer, R. E.; Shashidhar, R. E.; Calvert, J. M. Adv Mater 1997, 9, 61.
6. Chen, K. M.; Jiang, X.; Kimerling, L. C.; Hammond, P. T. Langmuir 2000, 16, 7825.
7. Zheng, H.; Rubner, M. F.; Hammond, P. T. Langmuir 2002, 18, 4505.
8. Otsu, T.; Kuriyama, A. Polym Bull (Berlin) 1984, 11, 135.
9. Otsu, T. J Polym Sci Part A: Polym Chem 2000, 38, 2121.
10. Ishizu, K.; Kojima, T.; Ohta, Y.; Shibuya, T. J Colloid Interface Sci 2004, 272, 76.
11. Ishizu, K.; Mori, A. Polym Int 2001, 50, 906.
12. Ishizu, K.; Mori, A. Macromol Rapid Commun 2000, 21, 665.
13. Fukunaga, K.; Elbs, H.; Magerle, R.; Krausch, G. Macromolecules 2000, 33, 947.
14. Segalman, R. A.; Hexemer, A.; Hayward, R. C.; Kramer, E. J. Macromolecules 2003, 36, 3272.
15. Tsubaki, K.; Ishizu, K. Polymer 2001, 42, 8387.
16. Katime, I.; Quintana, J. R. In Comprehensive Polymer Science; Booth, C., Price, C., Eds.; Pergmon: Oxford, 1989; Vol. 1, Chapter 5.
17. Thomas, H. R.; O'Malley, J. J. Macromolecules 1979, 12, 323.
18. Hasegawa, H.; Hashimoto, T. Macromolecules 1985, 18, 589.
19. Ishizu, K.; Fukuyama, T. Macromolecules 1989, 22, 244.
20. Ishizu, K.; Yamada, Y.; Fukutomi, T. Polymer 1990, 31, 2047.
21. Ishizu, K.; Yamada, Y.; Saito, R.; Kanbara, T.; Yamamoto, T. Polymer 1993, 34, 2256.
22. Ishizu, K.; Ohta, Y.; Kawauchi, S. J Appl Polym Sci, to appear.
23. Müller, A. H. E.; Yan, D.; Wulkov, M. Macromolecules 1997, 30, 7015.
24. Ishizu, K.; Ohta, Y.; Kawauchi, S. Macromolecules 2002, 35, 3781.
25. Ishizu, K.; Mori, A. Polym Int 2001, 51, 50.